MAGNETIC MEASUREMENT SYSTEM FOR THE SPARC INSERTION DEVICES

M. Quattromini, F. Ciocci, G. Dattoli, M. Del Franco, A. Doria,
G. P. Gallerano, L. Giannessi, E. Giovenale, A. Lo Bue, G. L. Orlandi, A. Petralia,
P. Rossi, L. Semeraro, I. Spassovsky, V. Surrenti, ENEA, 00044 Frascati, Italy
A. Dipace, E. Sabia, ENEA, 80055 Portici, Italy

Abstract

The characteristics and performances of the magnetic measurement system for the SPARC insertion devices are presented. A typical configuration formed by a a Hall probe mounted on a cart sliding on a granite beam was adopted to measure the properties of the six SPARC undulator sections. This approach is usually adopted for rapid local field measurements. In this contribution we show that precision levels comparable to those of other well established techniques can be achieved also for critical issues like alignments, field integrals, phase errors etc.

INTRODUCTION

The SPARC FEL is composed by an accelerator aimed at providing a high brightness electron beam in an energy range comprised between 150 and 200 MeV and a $12\,\mathrm{m}$ long, permanent magnets, variable gap undulator [1]. The laser driven, 1.6 cells, S-band SLAC/BNL/UCLA-type RF photo-injector and its performances are described elsewhere [2]. The final energy is achieved by means of three SLAC-type TW linac sections at 2.856 GHz. The first two sections are surrounded by solenoids providing additional focalization during acceleration.

The SPARC undulator consists of six identical sections, realized by ACCEL Instruments GmbH[3], whose characteristics are reported in Table 1. The permanent magnets are assembled according to the standard Halbach configuration. The gaps between contiguous sections accommodate quadrupoles for e-beam transport and matching, diagnostic chambers to assess both e-beam and FEL radiation properties, and magnetic correctors for compensation of the longitudinal dephasing between electrons and fields.

The SPARC FEL is aimed not only at operating in SASE regime, but also at studying seeding and non linear harmonics generation, which are sensitive to inhomogeneous broadening induced by magnetic field errors[4]. For these reasons, the fulfillment of design performances, namely saturation in a magnetic length smaller than $12\,\mathrm{m}$ and simultaneous operation at the fundamental and higher harmonics wavelengths poses fairly strict requirements on the magnetic field quality. Among others, two issues are of major concern:

- Accurate identification of the mechanical and magnetic axes and control of the gap tuning.
- Assessment of both transverse field components homogeneity and of field integrals calculated along the beam axis.

The apparatus set up to check fulfillment of design requirements in described in the next section, along with the procedures devised for accurate characterization and alignment.

Table 1: Undulator parameters

Period	$2.8\,\mathrm{cm}$
Undulator length	$2.156\,\mathrm{m}$
No. of periods	77
Gap (nom/min/max)	$0.858/0.6/2.5\,\mathrm{cm}$
K (nom/min/max)	$2.145/3.2/0.38$
Remnant field	$1.31\,\mathrm{T}$
Blocks per period	4
Block size (h×l×w)	$2 \times 0.7 \times 5\,\mathrm{cm}$

THE MEASURE WORKBENCH

The measurement bench is consisting of a Hall probe (Lakeshore model HMFT-3E03-VR) mounted on a movable cart, sliding over an air cushion on a $3\mathrm{m}$ long granite beam (parallel to the undulator section) whose top surface is polished to a flatness of $\pm 5\mu\mathrm{m}$ to reduce jolting. The cart is driven longitudinally by means of a gear wheel coupled to a cog rail mounted on the granite beam, controlled via a DC-servo motor drive with encoder PI mod. C136-10, which guarantees 1µm resolution. The longitudinal jitter/repeatability is estimated to $\pm 5\mu\mathrm{m}$.

Transverse motion is attained by means of a x-y translation stage (Physik Instrumente model M 521 equipped with non contact linear encoder) mounted on the cart. The Hall probe is placed on the tip of a conical, horizontal aluminum branch, mounted on the x-y stage. The stage linear table provides low friction, backlash-free positioning and guarantees $1\mu\mathrm{m}/100\mathrm{mm}$ straightness and flatness by using precision linear guiding rails with recirculating ball bearings.

All magnetic measurements have been carried out in a dedicated room with temperature control with a stability of $\pm 0.5^{\circ}C$. By means of an optical level (NAK2 by Leica) and a laser tracker (LTD 500 by Leica) an absolute horizontal plane has been defined in the hall and the granite block has been aligned to this plane with an error of $10\mu\mathrm{m}/\mathrm{m}$. A view of the SPARC undulator magnetic measurement system with one of the undulator sections is shown in fig. 1.

The following analytical form is assumed for the field's

Figure 1: The magnetic field measurement bench with one of the ACCEL undulator sections under test at ENEA Frascati Laboratories.

main component[5]:

$$B_y(x,y,z) = B_0 \cos(k_x x) \cosh(k_y y) \sin(k_u z) \quad (1)$$
$$\left(k_u^2 = k_y^2 - k_x^2\right)$$

In eq. (1) the field expression factorizes in the product of terms depending on a single variable. This property is exploited in the alignment procedure developed to determine the undulator magnetic axis, which consists essentially in scanning the undulator field's main ("B_y") component along the horizontal ("x") and vertical ("y") directions *separately*, at longitudinal ("z") positions corresponding to field's extrema ($|\sin(k_u z)| \approx 1$). For every longitudinal position, field data are fitted to an analytical expression of the type

$$\begin{aligned} B_y(x) &= \tilde{B} \cdot \cos[k_x (x - x_0)] \qquad (x \text{ scan}) \\ &\text{or} \\ B_y(y) &= \tilde{B} \cdot \cosh[k_y (y - y_0)] \qquad (y \text{ scan}) \end{aligned} \quad (2)$$

for the values of $\tilde{B}, k_{x(y)}$ and $x_0\,(y_0)$. A typical example is given in fig. 2 where the data collected at given longitudinal positions and the corresponding fits are superimposed for a scan along the horizontal (top) and vertical (bottom) coordinate. The comparison between the plots clearly shows the much stronger field dependence on the vertical coordinate with respect to the other transverse direction, where the field remain almost constant over several millimeters, reflecting the condition $k_x \ll k_y \approx k_u$. The local "center" positions ("x_0","y_0") at different values of z along the undulator are shown in fig. 3 along with fits to straight lines. The slopes of these fits for the x and y axes define the "yaw" and the "pitch" of the undulator, respectively, which are to be reduced by means of the control knobs available on the undulator's platform. The procedure is iterated until convergence is achieved, i.e. the yaw is within a fraction of mrad and the pitch within $10\mu\text{rad}$. A glimpse at the error bars in fig. 3 - which have been multiplied by a factor $10\times$ for clarity - suggests that the deviates between data

Figure 2: Typical fits (dashed lines) of $B_y$vs x (top) and $B_y$vs y (bottom) to functions in eq. (2).

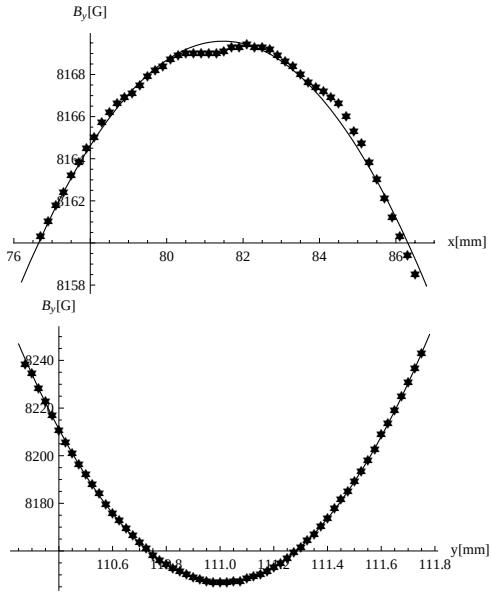

Figure 3: Fit of $x_0$vs$z$ (top) and $y_0$vs$z$ (bottom) to a straight line. The error bars have been amplified by a factor $10\times$ for clarity.

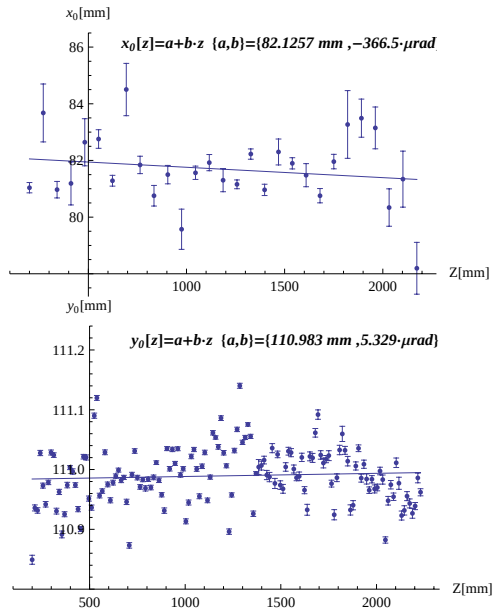

and the fit straight line are statistically meaningful, reflecting a genuine scattering in the local magnetic axis from one period to the other, in the sense that central positions may differ up to few mm (x_0) and few hundreds μm (y_0) in horizontal and vertical directions, respectively.

INTERFEROMETRIC MEASURE OF FIELD INTEGRAL

Once the magnetic axis has been identified, repeated longitudinal scans are taken to check whether the 1^{st} field integral is within specifications ($\int B_y(z)\,dz \leq 0.5\mathrm{G}\cdot\mathrm{m}$). In fig. 4 (top) is displayed the distribution of first integral for a sample of 28 scans for undulator's first section. The mean value is clearly larger than the maximum allowed in the specifications. The source of this result could be the longitudinal jitter of the longitudinal DC drive. For this reason the longitudinal positions are acquired by means of a dual-frequency laser interferometer JENAer ZLM700[6]. The distribution of first integral obtained this way (see fig. 4 (bottom)), exhibits a lower mean value and a comparable standard deviation. The dispersion in the data in both cases is fully understood in terms of the error figure of the Hall probe ($\epsilon \approx 2‰_{(\mathrm{read\ value})} + 1‰_{(\mathrm{full\ scale\ value})}$). The clustering of the two distributions around statistically well separated mean values suggests the presence of a systematic component in the overall error sources. This conjecture is confirmed by inspection of the deviates between longitudinal positions as measured by the digital encoder coaxial to the DC drive and the interferometer, which exhibits a remarkably steady pattern (see fig. 5 for an example) from one scan to the other. Clearly the estimation of field's 1^{st} integral based on position data from interferometer seems more reliable. To check this conjecture, the undulator section was displaced longitudinally by $\delta = -\lambda_{\mathrm{u}}/4, +\lambda_{\mathrm{u}}/4, +\lambda_{\mathrm{u}}/2$ and $+11\lambda_{\mathrm{u}}/18$ ($-90^{\mathrm{o}}, +90^{\mathrm{o}}, +180^{\mathrm{o}}$ and $+220^{\mathrm{o}}$). The field integrals evaluated with interferometric position data are expected to remain constant while those evaluated with encoder data are

Figure 4: Distribution of $\int B_y(z)\,dz$ for a sample of 34 scans using coordinatometer (top) and interferometer (bottom) data for longitudinal positions.

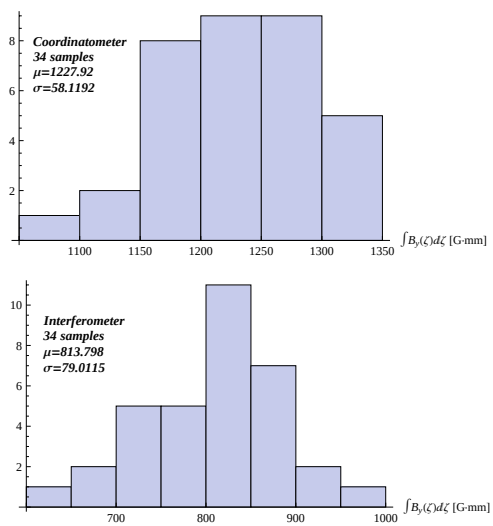

Figure 5: Plot of $\zeta_{\mathrm{coord}} - \zeta_{\mathrm{interf}}$ along the undulator.

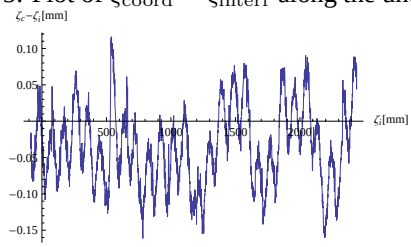

expected to oscillate around the "true" value with a period λ_{u}. This behaviour has been confirmed by data, as is clearly visible in fig. 6, where the encoder data oscillate around a value very close to the value - (almost independent on the displacement δ - obtained with interferometric data.

An enlarged version of this paper, is available at SPARC website[7].

Figure 6: Oscillation of field's 1^{st} integral evaluated with encoder data around the interferometer data. Solid line is a fit to $A + B\cdot\sin(k_{\mathrm{u}}\delta)$.

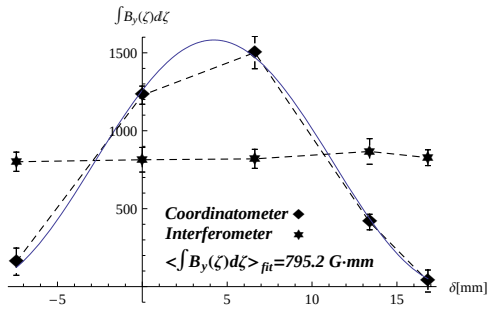

ACKNOWLEDGMENTS

We are pleased to thank D. Doelling, H.-U. Klein, D. Krischel, P. Komoroski, M. Meyers-Reumers and all technicians at ACCEL Intruments GmbH for the work done building SPARC undulator and kind support during testing and installation.

REFERENCES

[1] SPARC Collaboration, Nucl. Instr. & Meth. A507 (2003) 345-349, see also http://www.sparc.it

[2] M. Ferrario et al., Phys. Rev. Lett. 99, 234801 (2007).

[3] http://www.accel.de, see also D. Doelling et al., PAC'07, Albuquerque, July 2007, TUPMN010, http://www.JACoW.org.

[4] L. Poletto et al. Proceedings of FEL'06, BESSY, Berlin, Germany MOPPH028, http://www.JACoW.org.

[5] G. Dattoli, A. Renieri and A. Torre, Lectures on Free Electron Laser Theory and Related Topics, World Scientific (1993).

[6] See http://www.jenaer-mt.com/en/produkte/zlm800.php.

[7] AA.VV., SPARC Tech. note SPARC-FEL-08/001.